Study of Conducted EMI Reduction for Three-Phase Active Front-End Rectifier

Dong Jiang, Rixin Lai, Fei (Fred) Wang, *Fellow, IEEE*, Fang Luo, Shuo Wang, *Senior Member, IEEE*, and Dushan Boroyevich, *Fellow, IEEE*

***Abstract*—The problem of electromagnetic interference (EMI) plays an important role in the design of power electronic converters, especially for airplane electrical systems. This paper explores techniques to reduce EMI noise in three-phase active front-end rectifier. The Vienna-type rectifier is used as the object. The design approach introduced in this paper is using a high-density EMI filter to satisfy the EMI standard. Design methodology is introduced in the paper by a three-stage *LC–LC–L* filter structure. In particular, the cause of high noise at high frequencies is studied in experiments, and the coupling effect of the final-stage capacitor and inductors is investigated. In order to reduce the EMI noise in the mid-frequency range, the application of random pulsewidth modulation (PWM) is also presented. The performance of random PWM in a Vienna-type rectifier is verified by theoretical analysis and experimental results. The approaches discussed in this paper significantly reduce the EMI noise in the Vienna-type rectifier, and therefore, the filter size can also be reduced.**

***Index Terms*—Coupling, electromagnetic interference (EMI), random pulsewidth modulation (RPWM), Vienna-type rectifier.**

I. Introduction

POWER electronic converters are playing a more and more important role in three-phase ac power systems in industrial applications. By increasing the switching frequency, the converter can achieve better power quality with a smaller volume. However, a faster switching frequency will also introduce larger high-frequency voltage and current noise components to the system, which makes the electromagnetic compatibility (EMC) an important concern [1], [4]. Electromagnetic interference (EMI) noise can interfere with the electronic system in critical control and communication functions, which has an impact on the system reliability. In some applications with a high reliability requirement, like aircraft and aerospace electrical systems, EMC is especially important, since much less interference can be tolerated. In order to satisfy the reliability requirements, an EMI filter must be applied to reduce the noise. But on the other hand, high density is usually another essential requirement in those systems. Therefore, the power density of the whole converter considering the EMI filter has been studied in the recent years [1], [3], [4]. In order to increase the system power density, ways of reducing EMI noise without increasing filter volume/weight should be studied.

Active front-end rectifiers are developed as high performance ac–dc converters which can achieve high power quality in the ac side and close-loop controlled dc voltage. Since the high-frequency switching in the active switches in the active front-end rectifier, its EMI problem should be paid attention to, and is different from inverter. Among the different topologies of the three-phase ac–dc converter, the nonregenerative Vienna-type rectifier can perform with a three-level voltage waveform for input phase voltage and realizes unity power factor using only six active switches [1], [3]–[5]. The EMI noise of the Vienna-type rectifier is different from that of a normal two-level voltage source rectifier. Heldwein and colleagues [1], [4] analyze the input filter topology of the Vienna-type rectifier, and study the design methodology of the filter, including the DM and CM filter equivalent circuit and attenuation requirement. Lai *et al*. [3] give a design example of the filter for a 10-kW Vienna-type rectifier. However, none of these papers study the EMI reduction based on the physical structure of the filter, nor do they suggest a method to reduce EMI noise using pulsewidth modulation (PWM) strategies without changing filter size.

In the high-frequency range, a designed filter will lose its original performance as an ideal *LC* filter because of the parasitic components. Wang *et al*. [6], [7] studied the principle of parasitic components in the *LC* filter in dc–dc converters and parasitic cancelling methods, [8] studied winding capacitance cancelling for a three-phase converter, but did not study the coupling inductance. The problem of EMI in the high-frequency range EMI problem of Vienna-type rectifiers needs further study with experiments.

For the mid-frequency range of EMI, parasitic components are not obvious and the *LC* filter will have the designed attenuation. In order to reduce the EMI noise without changing the filter, random PWM (RPWM) methods can be used [9]–[14], [16], [17]. The principle of RPWM is to spread the energy concentrated around the harmonics of switching frequency to a wider frequency range to reduce the EMI peak. Most of the

Manuscript received January 30, 2010; revised April 7, 2010; accepted June 1, 2010. Date of current version December 6, 2011. This paper was presented at the 2010 International Power Electronics Conference as an organized session paper, in Sapporo, Japan, June 2010, and it has been revised prior to its submission for consideration to the IEEE Transactions on Power Electronics. Recommended for publication by Associate Editor P. Tenti.

D. Jiang, F. Luo, and D. Boroyevich are with The Bradley Department of Electrical and Computer Engineering, Virginia Tech, Blacksburg, VA 24061 USA (e-mail: jiang@vt.edu; fangluo@vt.edu; dushan@vt.edu).

R. Lai is with the GE global research center Niskayuna, NY 12308 USA (e-mail: lairixin@vt.edu).

F. Wang is with The Min H. Kao Department of Electrical Engineering and Computer Science, The University of Tennessee, Knoxville, TN 37996 USA (e-mail: fred.wang@utk.edu).

S. Wang is with the Electrical Power Systems, GE Aviation, Vandalia, OH 45377 USA (e-mail: shuowang@ieee.org).

Color versions of one or more of the figures in this paper are available online at http://ieeexplore.ieee.org.

Digital Object Identifier 10.1109/TPEL.2010.2053219

0885-8993/$26.00 © 2011 IEEE

Authorized licensed use limited to: University of Florida. Downloaded on December 30,2020 at 05:33:09 UTC from IEEE Xplore. Restrictions apply.

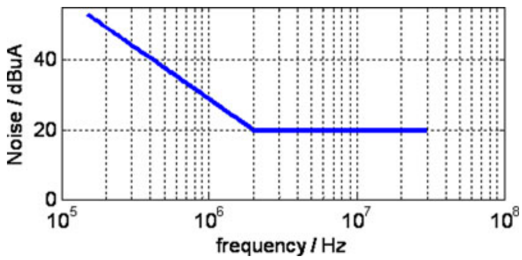

Fig. 1. D6-16050-5 EMI standard.

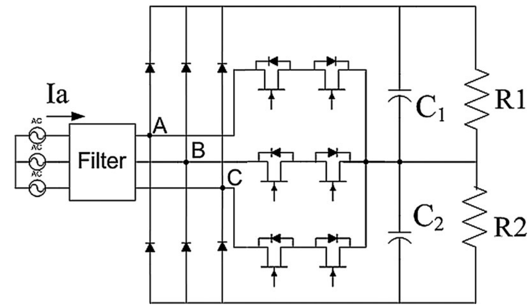

Fig. 2. Vienna-type rectifier based on SiC devices.

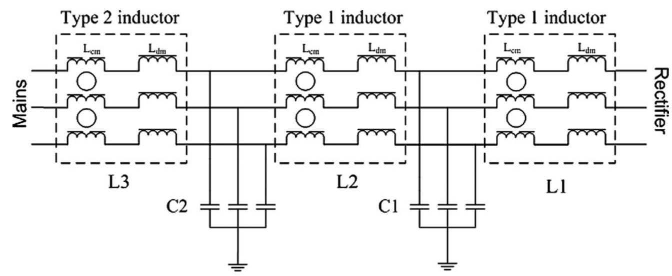

Fig. 3. Three-stage *L–CL–CL* filter.

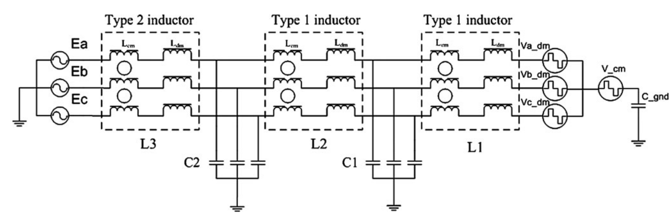

Fig. 4. Noise conducting path in the Vienna-type rectifier input filter.

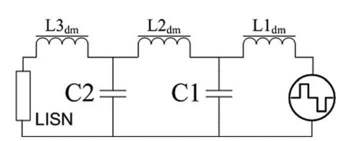

Fig. 5. DM filter equivalent circuit.

research (see [9]–[14]) on RPWM has been done with an inverter and with spectrum analysis in frequency ranges lower than 100 kHz. Kaboli *et al.* [17] analyzed the benefit of RPWM for single-switch power factor correction for diode rectifier. Kaboli *et al.* [16] applied RPWM techniques in Vienna-type of rectifier. However, it did not do theoretical analysis for the spectrum of RPWM and constant switching frequency PWM to make a comparison, nor did it make systematically comparison between RPWM and constant switching frequency PWM with experimental results. What is more, the noise frequency it studied is only up to 100 kHz, far less than the conducted EMI frequency range. For Vienna-type rectifiers, a theoretical analysis of the spectrum with RPWM needs to be performed, and an experimental comparison should be made of EMI noise when using different PWM strategies. Also, when RPWM is applied in Vienna-type rectifiers, the influence of RPWM on the power quality of the current is also unclear and needs to be studied.

In this paper, the EMI noise reduction of Vienna-type rectifier is studied. A three-stage *LC–LC–L* filter structure is used for the Vienna-type rectifier. The influence of parasitic components in the *LC* filter on the high-frequency EMI noise is studied. The use of RPWM in the Vienna-type rectifier is also studied.

In this paper, the narrowband EMI standard D6-16050-5 is used [2]; this is shown in Fig. 1. The frequency range is 150 kHz–30 MHz, and the current bandwidth should be selected to be between 1 and 3 kHz, according to the standard. In the experiment, 1-kHz bandwidth is selected for EMI measurement. The sampled current in the transmission line is transferred to dBμA and compared with the standard.

Section II introduces a design example of an input filter for a Vienna-type rectifier, including the physical design and an EMI testbed is set up. Then, in Section III, the problem of EMI noise in the high-frequency range is studied with experimental results. Theoretical analysis and experiments for the reduction of EMI noise in Vienna-type rectifiers in the mid-frequency range are discussed in Section IV. Conclusions are made in Section V.

II. Design of the EMI Filter

A Vienna-type rectifier is shown in Fig. 2. To achieve a high switching frequency, SiC Schottky diodes and SiC JFETs are used as the switches. Two 35-μF film capacitors are connected in the dc bus and load resistors are also connected in the dc bus. The maximum dc bus voltage is 650 V, with 230 V (RMS) input phase-neutral voltage and the maximum power is 10 kW.

Based on the analysis in [3], a three-stage *L–CL–CL* input filter is designed to satisfy the EMI standard, as shown in Fig. 3. The two *CL* filters have the same parameters and the same corner frequency f_R. 1-μF film capacitors are used in the filter. A three-phase inductor with a nanocrystalline core is used as the inductor in the filter. Its three-phase main inductance serves as CM inductance and the leakage inductance serves as DM inductance. The equivalent EMI path of the input filter of the Vienna-type rectifier is shown in Fig. 4. The noise sources are the pulsating voltage in the rectifier terminals. The noise source can be divided into two groups: CM noise source and DM noise sources, as shown in (1). The DM noise only goes through the ac lines; the equivalent filter path is shown in Fig. 5. The CM noise source generates conducted EMI going through the parasitic capacitor to the ground. The grounding capacitor is mainly caused by the parasitic capacitance between switch and heat sink. For the worst case, the neutral point of the dc link is directly connected to the ground. The equivalent circuit of the

Authorized licensed use limited to: University of Florida. Downloaded on December 30,2020 at 05:33:09 UTC from IEEE Xplore. Restrictions apply.

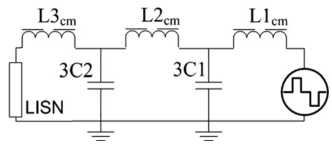

Fig. 6. CM filter equivalent circuit.

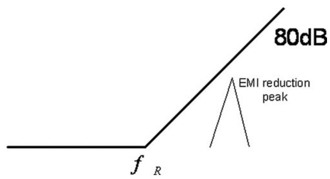

Fig. 7. Two-stage filter damping principle.

CM filter is shown in Fig. 6. The DM and CM corner frequency of the last two stage filters can be calculated as $L_{\mathrm{dm}}C$ and $3L_{\mathrm{cm}}C$, L_{dm}, and L_{cm} are the CM and DM inductance of L1 and L2. Equation (2) describes the approximate relationship between the capacitance and inductance of *CL* filter, both for CM and DM noises.

$$\begin{cases} V_{\mathrm{CM}} = \dfrac{V_a + V_b + V_c}{3} \\ V_{\mathrm{DM}} = V_{(a,b,c)} - V_{\mathrm{CM}} \end{cases} \tag{1}$$

$$\begin{cases} L_{\mathrm{dm}} = \left(\dfrac{1}{2\pi f_{R\_\mathrm{dm}}}\right)^2 \dfrac{1}{C} \\ L_{\mathrm{cm}} = \left(\dfrac{1}{2\pi f_{R\_\mathrm{cm}}}\right)^2 \dfrac{1}{3C}. \end{cases} \tag{2}$$

The PWM spectral voltage is calculated by double-Fourier analysis of the converter terminal voltage [3]. *CL–CL* filters have 80-dB attenuation characteristics; the corner frequency can be calculated by spectral and EMI requirements, and the principle is shown in Fig. 7. Lai *et al.* [3] show the calculated corner frequency for DM and CM filters with different switching frequencies and propose that with 40 and 70 kHz, switching frequencies are preferred since the corresponding filter corner frequency can be big. 12-mH CM inductance and 100-μH DM inductance are designed.

High permeability, high saturating flux nanocrystalline toriod core is selected to be used as the core for the inductor. The dimension of the toriod core is shown in Fig. 8. With the dimension, the area of the cross section A_c and the equivalent core length l_e can be calculated in (3). With the dimension parameters and the turns N, the CM and DM inductance of the inductor with toriod core can be calculated in (4) and (5) [15]. In (5), θ_1 is the angle of the arc of one phase winding

$$\begin{cases} A_c = \dfrac{1}{2}(a-b)c \\ l_e = \pi(a+b) \end{cases} \tag{3}$$

$$L_{\mathrm{CM}} = \frac{\mu_0 \mu_r A_c N^2}{l_e} \tag{4}$$

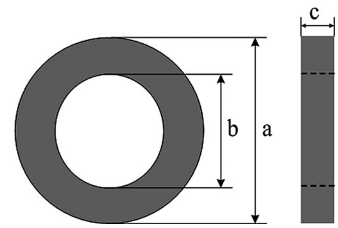

Fig. 8. Dimension of toriod core.

$$L_{\mathrm{DM}} = \begin{cases} \mu_{\mathrm{eff}} \dfrac{\mu_0 N^2 A_c}{l_e \sqrt{(\theta_1/360) + (\sin(\theta_1/2)/\pi)}} (\text{one layer}) \\ 0.5 \times \mu_{\mathrm{eff}} \dfrac{\mu_0 N^2 A_c}{l_e \sqrt{(\theta_1/360) + (\sin(\theta_1/2)/\pi)}} (\text{two layers}) \end{cases}$$
$$\left(\mu_{\mathrm{eff}} = 2.5 \left(\sqrt{\frac{\pi}{A_c}} \frac{l_e}{2}\right)^{1.45}\right). \tag{5}$$

Knowing the inductance and current rating, a nanocrystalline core is selected for the inductor, shown in Fig. 9(a), with 6.2-cm outer diameter and 1.1-cm height. For the *CL*-stage filter, double-layer copper wire is used to achieve 100-μH DM inductance and 12-mH CM inductance; this is called type 1 inductor, and is shown in Fig. 9(b). However, the double-layer copper wire has big parasitic capacitance which will significantly influence the equivalent inductance of the *CL* filter at high frequencies (2–30 MHz), which is in EMI range. In fact, CM noise plays the main role in the high-frequency range, so a type 2 inductor will be the last stage filter for the three-stage filter, with a single layer of wire with plastic coating, which can significantly decrease the parasitic capacitance. This type 2 inductor is shown in Fig. 9(c).

To verify the EMI filter performance, experiments are done using schematic in Fig. 2. Three line impedance stabilization networks (LISNs) are connected between the three-phase ac source and the power converter. In the experiment, 115-V (phase neutral, RMS) ac input voltage and 330-V dc voltage is used. For the load resistor, $R1 = R2 = 15\ \Omega$. For the controller, a 300-Hz bandwidth voltage loop and a 2000-Hz bandwidth current loop is used. Experiments are done with an SiC Vienna-type rectifier with the designed three-stage filter. A type 8616-5-TS-200-N LISN is applied to the input side for EMI measurement.

III. Improvement of Noise Reduction in the High-Frequency Range

All of the designs are based on the ideal model of inductor and filter. However, the parasitic parameters embedded in the components will influence the filter performance, especially in the high-frequency range. The most important issue is the equivalent series inductance (ESL) in the final-stage capacitor, as shown in Fig. 10. There are couplings between the ESL of $C2$ and $L1$ and $L2$. Because the noise in the inductor is much bigger than the noise in $C2$, even though the coupling inductance is very small, it will significantly influence the filtering performance of the filter. Fig. 11 shows the three-stage filter attenuation curve when there is 100-pH coupling between $C2$ and

Authorized licensed use limited to: University of Florida. Downloaded on December 30,2020 at 05:33:09 UTC from IEEE Xplore. Restrictions apply.

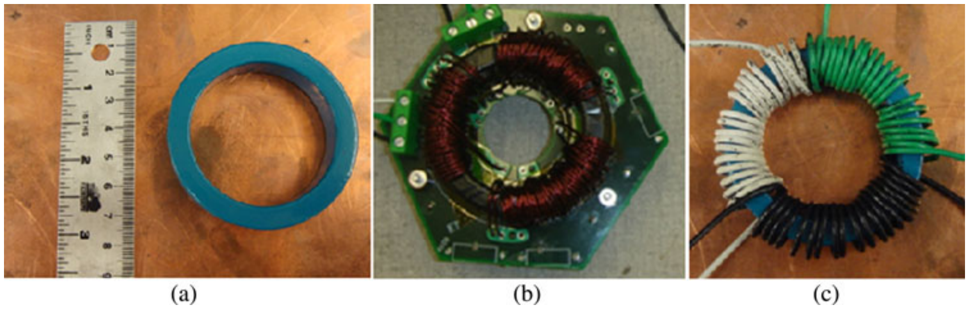

Fig. 9. (a) Nanocrystalline core, (b) type 1 inductor, and (c) type 2 inductor.

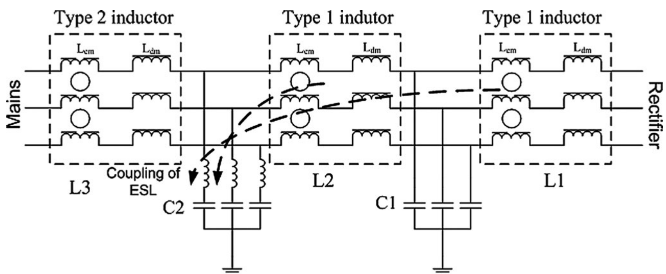

Fig. 10. Coupling in the three-stage filter.

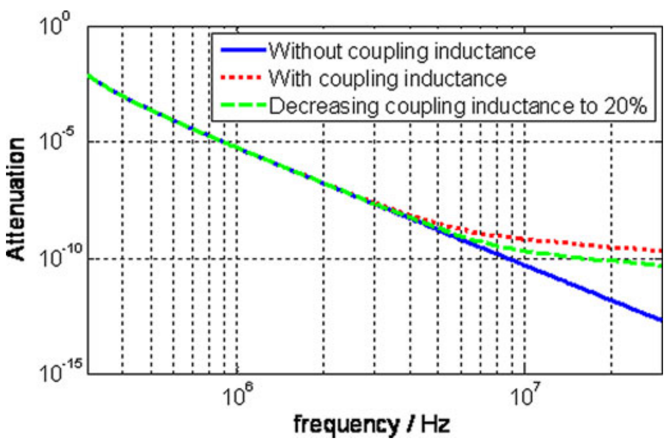

Fig. 11. Influence of coupling inductance on attenuation.

TABLE I
THEORETICAL TERMINAL PHASE VOLTAGE OF VIENNA-TYPE RECTIFIER IN EACH SWITCHING CYCLE

	$\frac{1-d}{2}T_s < t < \frac{1+d}{2}T_s$	$t < \frac{1-d}{2}T_s$ or $t > \frac{1+d}{2}T_s$	
I_{in}	Either >0 or <0	>0	<0
V_{in}	0	$\frac{V_{dc}}{2}$	$-\frac{V_{dc}}{2}$

$L2$ and 10-pH coupling between $C2$ and $L1$, in high-frequency range (10–30 MHz), the attenuation with the coupling has more than 20-dB error than the ideal filter. If the coupling inductance can be decreased to 20%, the attenuation can be improved more than 10 dB.

The setup of the filter (without $L3$) in the experiment is shown in Fig. 12. In Fig. 12(a), the last-stage capacitor ($C2$) is put on the same side as $L2$, which means it is close to the inductor. In Fig. 12(b), $C2$ is put on the side opposite from $L2$, the coupling inductance is reduced. In Fig. 12(c), $C2$ is put on an extra board, which means the coupling inductance between $L2$ and $C2$ is largely reduced. EMI is measured using the same voltage rating (330 V) and switching frequency (70 kHz), and these measurements are displayed in Fig. 13. In the mid-frequency (150 kHz–10 MHz) range, there is no big difference in EMI for the three cases. However, when the frequency is in high-frequency range, a significant EMI peak appears in case (a) since the coupling influence is big. When the capacitor is put on the opposite side, the high-frequency EMI peak can reduce a little and is under the standard's limit. When the C2 is put on an extra board, the high-frequency EMI peak will be significantly reduced.

This comparison shows that the coupling inductance between inductor and the last-stage capacitor is the main reason for the high-frequency EMI peak. In the lay out of the filter, this influence is very important. Further improvement like the magnetic isolation should be considered of.

IV. Improvement of Noise Reduction in Mid-Frequency Range

In the mid-frequency range (150 kHz–10 MHz), the linearity of the input filter stays nearly the same as the designed value. The method for reducing the EMI noise will not be based on parasitic parameters. Constant switching frequency space-vector pulsewidth modulation (SVPWM) is applied in the rectifier. As displayed in Fig. 13, obvious oscillation in the EMI noise can be found. The peak of the EMI noise is close to the standard. This is because that the power of the switching voltage is focused near the harmonics of the switching frequency. When designing the EMI filter, the corner frequency is selected to meet the requirement of the worst case. In order to minimize the size of the filter, the switching frequency is selected in [3]. 70 kHz and 140 kHz are selected since they can push the filter corner frequency to be high and satisfy the EMI standard. For a 70-kHz switching frequency, the second-order harmonic of the switching frequency (140 kHz) can avoid the EMI standard's lower limit (150 kHz). However, the higher harmonics of the switching frequency still produce the worst EMI noise, shown by Fig. 13.

Random PWM (RPWM) is an improved SVPWM method using a nonconstant switching frequency. By changing the

Authorized licensed use limited to: University of Florida. Downloaded on December 30,2020 at 05:33:09 UTC from IEEE Xplore. Restrictions apply.

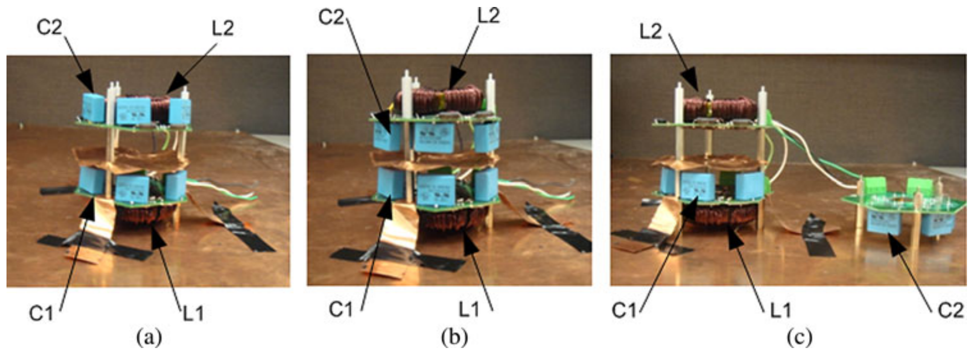

Fig. 12. Three different setup of the filter: (a) $C2$ close to inductor, (b) $C2$ on different side from $L2$, and (c) $C2$ far away from the inductor.

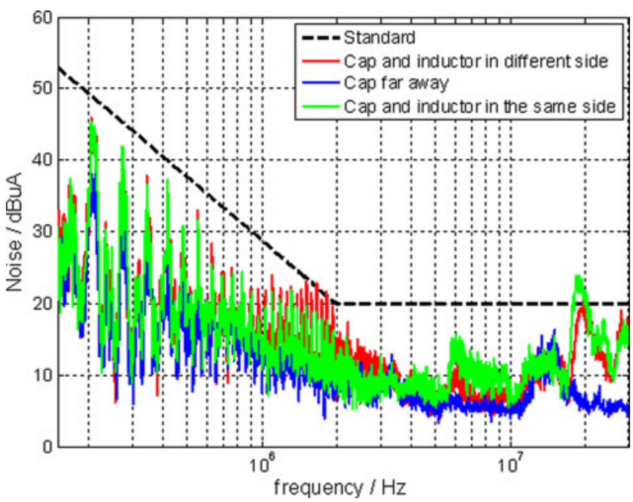

Fig. 13. Comparison of the EMI in the three different setups of the filter.

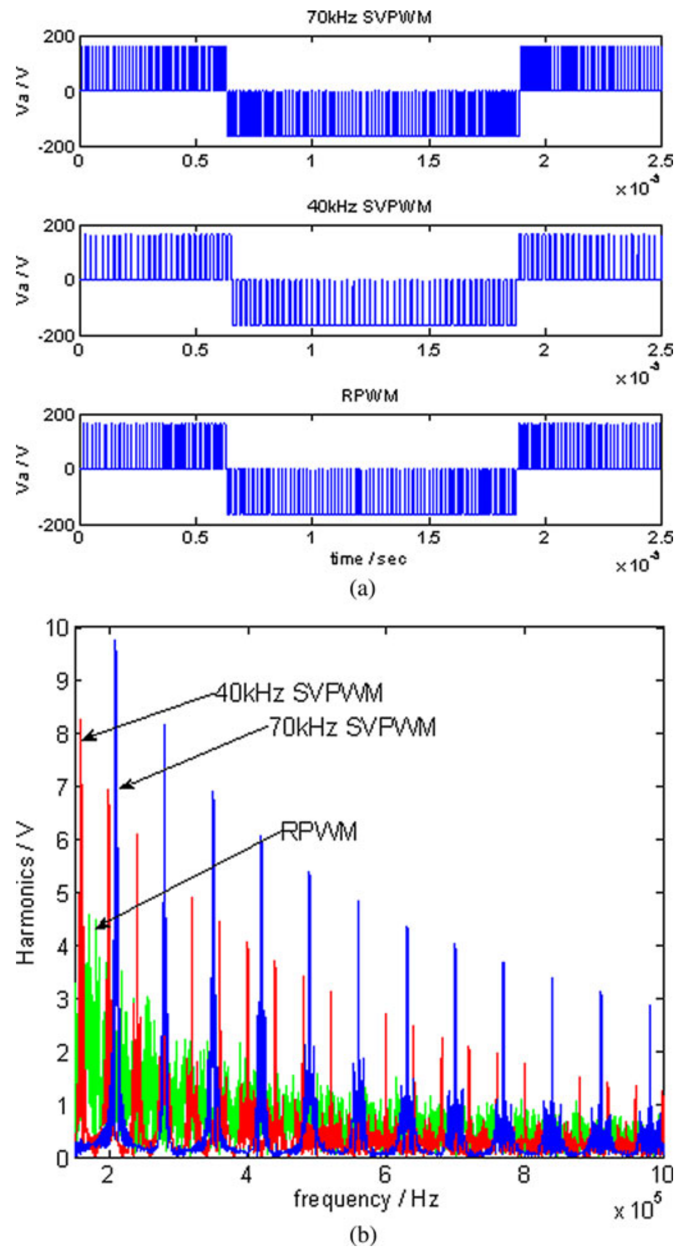

Fig. 14. Theoretical calculation results of phase voltage of Vienna rectifier with 70-kHz SVPWM, 40-kHz SVPWM, and RPWM (55–70 kHz): (a) Waveform and (b) spectrum.

switching frequency, the noise energy will be spread in a wider frequency range and the peak noise in the harmonics of the switching frequency will be reduced. This idea has been applied to inverters [9]–[14]. By applying this idea to high-frequency Vienna-type rectifiers, the input current EMI noise peak can also be reduced. The switching frequency should vary within a range much higher than the current controller frequency so the RPWM method will not influence the low frequency component of the current. It will also not impair the power quality of the current.

In order to verify the function of RPWM, theoretical Fourier analysis has been done for a phase-voltage waveform. The phase voltage in the Vienna-type rectifier is determined by the switching function, shown in Table I. In the table, d is the duty cycle of the gate signal in the switching period T_s. In each switching period, the terminal voltage of the rectifier can be 0 and $\pm V_{\mathrm{dc}}/2$, which is determined by the gate signal and current direction. A waveform of the terminal phase voltage of one line period in a Vienna-type rectifier can be constructed by this table, with 330-V dc bus voltage, 110 V (RMS) input voltage and unity power factor, with both constant switching frequency and random switching frequency. The waveforms of the phase voltage are displayed in Fig. 14(a), using one line cycle data. Using Fourier analysis to calculate the spectrum of the phase voltage

Authorized licensed use limited to: University of Florida. Downloaded on December 30,2020 at 05:33:09 UTC from IEEE Xplore. Restrictions apply.

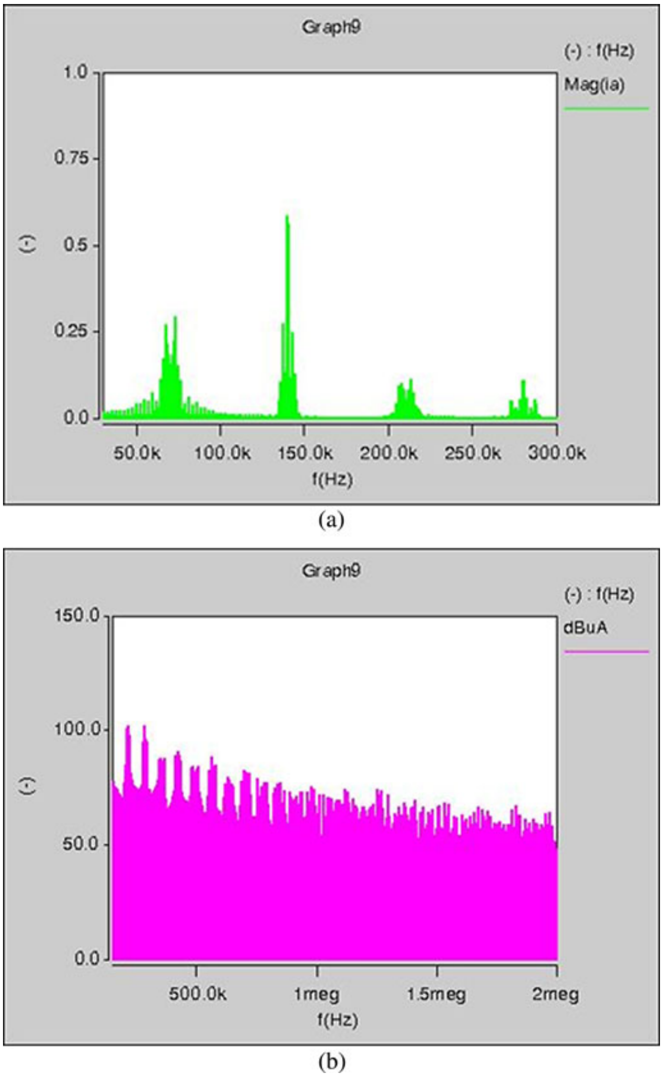

Fig. 15. Simulation results of current spectrum in Ampere and dBμA of the Vienna rectifier with only boost inductor and using 70-kHz SVPWM.

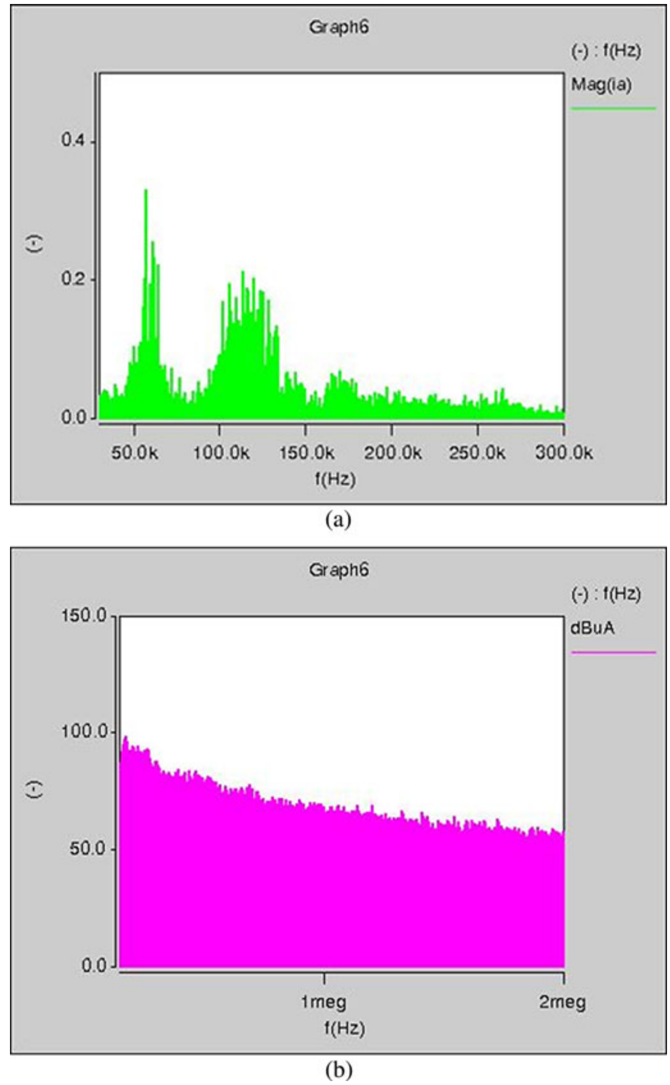

Fig. 16. Simulation results of current spectrum in Ampere and dBμA of the Vienna rectifier with only boost inductor and using 55–70-kHz RPWM.

from 150 kHz to 1 MHz, the results are shown in Fig. 14(b). The spectrum of 70-kHz SVPWM is concentrated in integers of 70 kHz, with the 9.7-V maximum value near 210 kHz. The spectrum of 40-kHz SVPWM is concentrated in integers of 40 kHz, with the 8.2-V maximum value near 160 kHz. However, with the RPWM switching frequency ranging from 55 to 70 kHz, the noise spreads out in a wider frequency range and the maximum voltage is less than 5 V. With an input filter, the theoretical EMI noise with the RPWM can be less than SVPWM in the mid-frequency range.

A similar conclusion is found with Saber simulation results, shown in Figs. 15 and 16. The simulation was performed with 330-V dc bus voltage, 5-kW load, and 70-kHz switching frequency. Using only a 100-μH input inductor and no extra filter, the spectrum of the input current around the EMI lower limit is shown in Fig. 15(a). Although the 140-kHz spectrum peak avoids the EMI range, the current noise peak (in dBμA) in the EMI range still has obvious peak in 210 and 280 kHz, the EMI is up to 100 dB. Fig. 16 shows simulation results when using RPWM ranging from 55 to 70 kHz. The current spectrum is distributed continuously, and the noise in the EMI frequency range is much smoother than it is with constant frequency SVPWM, it is about 10 dB less around 280 kHz.

In order to verify the performance of RPWM in Vienna-type rectifier, experiments are performed. In the beginning of the DSP program, an N random numbers ranging between 0 and 1 is generated by MATLAB and saved as *rand[N]*. At the beginning of the interruption program, the PWM cycle is updated using (6) with a changing index between 1 and N. PWM_cycle0 is the PWM cycle of the initial switching frequency f_0. With the defined coefficient λ, the switching frequency will change between $f_0/(1 + \lambda)$ and f_0 so the random PWM range can be changed with f_0 and λ. If PWM_cycle0 is defined as 1.4286×10^5 s (70 kHz), and coefficient $\lambda = 0.2727$, the switching frequency will change between 55 and 70 kHz. If $\lambda = 0$, the switching

Authorized licensed use limited to: University of Florida. Downloaded on December 30,2020 at 05:33:09 UTC from IEEE Xplore. Restrictions apply.

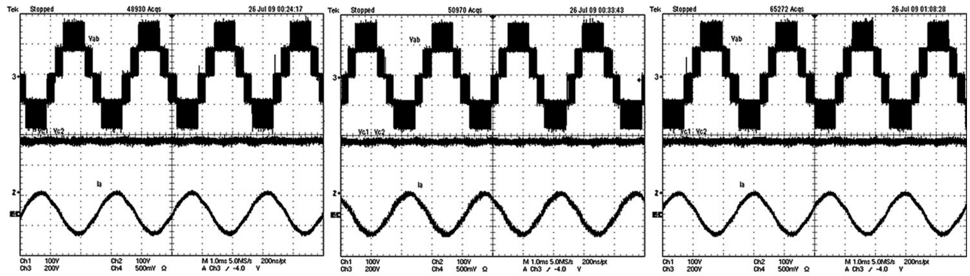

Fig. 17. Experimental results of Vienna-type Rectifier with (a) 70-kHz SVPWM, (b) 40-kHz SVPWM, and (c) 55–70-kHz RPWM.

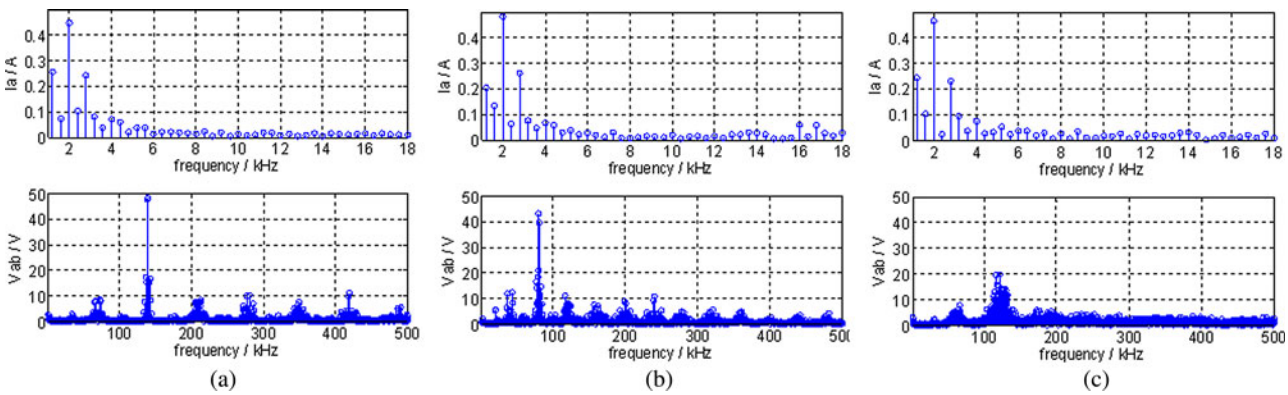

Fig. 18. Fourier analysis results of the current and voltage of Vienna-type rectifier: (a) with 70-kHz SVPWM, (b) 40-kHz SVPWM, and (c) 55–70-kHz RPWM.

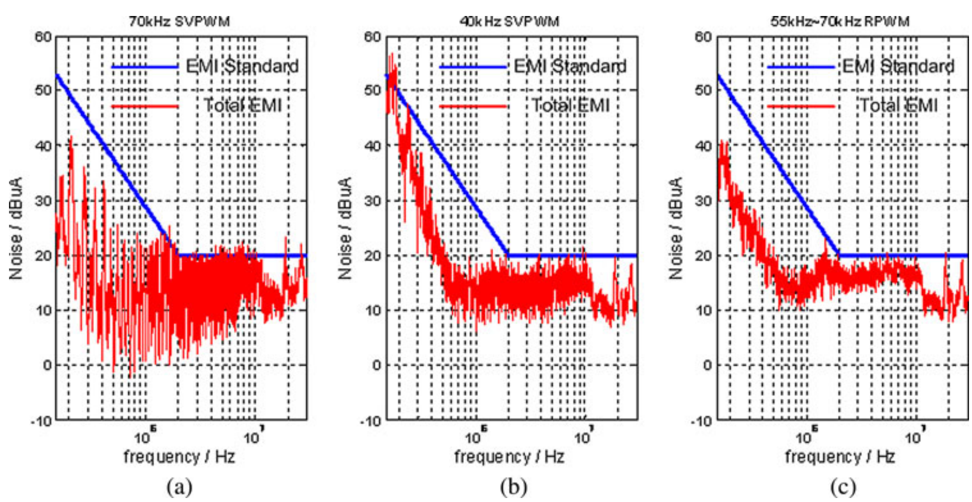

Fig. 19. Experimental results: EMI measurement results of three cases with three-stage filter, 330-V dc voltage and 3.6-kW output power.

frequency will be fixed at 70 kHz.

$$\mathrm{PWM\_cycle} = \mathrm{PWM\_cycle0} \times (1 + \lambda \times \mathrm{rand[index]}). \quad (6)$$

The experimental results are shown in Figs. 17–19. Fig. 17 displays the experimental results of the Vienna-type rectifier with 70-kHz SVPWM and RPWM ranging from 55 to 70 kHz, using random data number $N = 200$. The waveforms are similar for both the PWM methods. The line–line voltage V_{ab} of the rectifier input voltage is a five-level PWM waveform with a 660-V peak–peak value. The dc-link voltages (V_{c1}, V_{c2}) are controlled with error less than 3 V. The input phase currents (take phase A as example) in the three cases have the same fundamental value (25 A/div). Their low-order harmonics (1–18 kHz) are displayed in Fig. 18. The low-order harmonics are similar in the three cases, with the 2-kHz value (fifth-order harmonic) as the biggest, and the peak current harmonic is less than 0.5 A. This is because the control bandwidth is much less than the switching frequency and the methods used with PWM have very little influence on the low-order harmonics. RPWM can perform with similar power quality to constant frequency SVPWM. The spectrums of line-to-line voltage in the three cases are displayed in Fig. 18. With 70- and 40-kHz SVPWM, the integers of the switching frequency have obvious harmonic peaks among the frequency range, with peak value more than

Authorized licensed use limited to: University of Florida. Downloaded on December 30,2020 at 05:33:09 UTC from IEEE Xplore. Restrictions apply.

40 V in the second-order harmonic. However, with RPWM, the voltage spectrum can be smoothly distributed in the frequency range, with a peak value less than 20 V.

Using an EMI tester, the current EMI noises in three different cases are measured and shown in Fig. 19. The results are measured using a spectrum analyzer with 1-kHz bandwidth and using the peak mode. At 70-kHz SVPWM (a) and 40-kHz SVPWM (b), the EMI noises have obvious oscillation in the mid-frequency range. This is because the EMI peak is concentrated around the harmonics of switching frequency. However, with RPWM, although the average EMI noise is similar with the constant frequency SVPWM, the oscillation of EMI is much less in RPWM, which keeps the EMI noise below the standard.

V. Conclusion

For modern power electronics converters with high switching frequencies, the EMI problem should be examined, especially for applications that require high reliability, like aircraft and aerospace applications. This paper studies EMI reduction of active front-end rectifiers, using the Vienna-type rectifiers as an example. The EMI noise reduction methods are based on the three-stage *LC* filter structure. The following conclusions can be made.

1) The EMI reduction requirements can be calculated by spectrum analysis of the voltage and the corner frequency of the filter can be calculated and the ideal L and C value can be decided. However, parasitic capacitance in the double-layer inductor windings is detrimental to the performance of the inductors at high frequencies. The third-stage inductor should serve as a CM choke for high-frequency CM noise reduction, with single-layer winding and with plastic coating.
2) In the high-frequency range, experimental results prove that the coupling inductance in the filter will significantly influence the EMI reduction result in the final-stage capacitor. The coupling between the final-stage capacitor and the two inductors should be reduced.
3) After theoretical analysis of different PWM methods based on the switching function of Vienna-type rectifiers, we determine that random PWM can spread the energy concentrated around the harmonics of switching frequency to a wider range than constant frequency SVPWM, and random PWM can decrease the noise peak. Experimental results prove that when using random PWM, the peak EMI noise in mid-frequency range can be reduced without a significant reduction in the power quality.

Acknowledgment

The authors would like to thank Boeing Company for supporting the research. The authors also would like to thank J. Francis from Virginia Tech for building the controller for experiment.

References

[1] M. L. Heldwein and J. W. Kolar, "Impact of EMC filters on the power density of modern three-phase PWM converters," *IEEE Trans. Power Electron.*, vol. 24, no. 6, pp. 1577–1588, Jun. 2009.
[2] *Electromagnetic Interference Control Requirements for Composite Airplanes*, EMI D6-16050-5, Aug. 2004.
[3] R. Lai, F. Wang, R. Burgos, Y. Pei, D. Boroyevich, B. Wang, T. A. Lipo, V. D. Immanuel, and K. J. Karimi, "A systematic topology evaluation methodology for high-density three-phase PWM AC–AC converters," *IEEE Trans. Power Electron.*, vol. 23, no. 6, pp. 2665–2680, Nov. 2008.
[4] M. L. Heldwein, "EMC filtering of three-phase PWM converters," Ph.D. dissertation, ETH, Zurich, Switzerland, 2008.
[5] R. Lai, F. Wang, R. Burgos, and D. Boroyevich, "Voltage balance control of non-regenerative three-level boost rectifier using carrier-based pulse width modulation," in *Proc. IEEE Power Electron. Spec. Conf.*, Jun. 15–19, 2008, pp. 3137–3142.
[6] S. Wang, F. C. Lee, W. G. Odendaal, and J. D. van Wyk, "Improvement of EMI filter performance with parasitic coupling cancellation," *IEEE Trans. Power Electron.*, vol. 20, no. 5, pp. 1221–1228, Sep. 2005.
[7] S. Wang, F. C. Lee, and J. D. van Wyk, "A study of integration of parasitic cancellation techniques for EMI filter design with discrete components," *IEEE Trans. Power Electron.*, vol. 23, no. 6, pp. 3094–3102, Nov. 2008.
[8] M. L. Heldwein and J. W. Kolar, "Winding capacitance cancellation for three-phase EMC input filters," *IEEE Trans. Power Electron.*, vol. 23, no. 4, pp. 2062–2074, Jul. 2008.
[9] T. G. Habetler and D. M. Divan, "Acoustic noise reduction in sinusoidal PWM drives using a randomly modulated carrier," *IEEE Trans. Power Electron.*, vol. 6, no. 3, pp. 356–363, Jul. 1991.
[10] A. M. Trzynadlowski, F. Blaabjerg, J. K. Pedersen, R. L. Kirlin, and S. Legowski, "Random pulse width modulation techniques for converter-fed drive systems—A review," *IEEE Trans. Ind. Appl.*, vol. 30, no. 5, pp. 1166–1175, Sep./Oct. 1994.
[11] C. B. Jacobina, A. M. N. Lima, E. R. C. da Silva, and A. M. Trzynadlowski, "Current control for induction motor drives using random PWM," *IEEE Trans. Ind. Electron.*, vol. 45, no. 5, pp. 704–712, Oct. 1998.
[12] A. M. Trzynadlowski, M. M. Bech, F. Blaabjerg, J. K. Pedersen, R. L. Kirlin, and M. Zigliotto, "Optimization of switching frequencies in the limited-pool random space vector PWM strategy for inverter-fed drives," *IEEE Trans. Power Electron.*, vol. 16, no. 6, pp. 852–857, Nov. 2001.
[13] A. M. Trzynadlowski, K. Borisov, Y. Li, and L. Qin, "A novel random PWM technique with low computational overhead and constant sampling frequency for high-volume, low-cost applications," *IEEE Trans. Power Electron.*, vol. 20, no. 1, pp. 116–122, Jan. 2005.
[14] K. Borisov, T. E. Calvert, J. A. Kleppe, E. Martin, and A. M. Trzynadlowski, "Experimental investigation of a naval propulsion drive model with the PWM-based attenuation of the acoustic and electromagnetic noise," *IEEE Trans. Ind. Electron.*, vol. 53, no. 2, pp. 450–457, Apr. 2006.
[15] M. J. Nave, "On modeling the common mode inductor," in *Proc. IEEE Int. Symp. Electromagn. Compat.*, Aug. 12–16, 1991, pp. 452–457.
[16] S. Kaboli, A. H. Rajaei, and A. Sheikhi, "Application of random PWM techniques for reducing the electromagnetic interference of Vienna rectifiers in distribution power system," in *Proc. IEEE 6th Int. Power Electron. Motion Control Conf.*, May 17–20, 2009, pp. 998–1003.
[17] S. Kaboli, J. Mahdavi, and A. Agah, "Application of random PWM technique for reducing the conducted electromagnetic emissions in active filters," *IEEE Trans. Ind. Electron.*, vol. 54, no. 4, pp. 2333–2343, Aug. 2007.
[18] H. Akagi and T. Shimizu, "Attenuation of conducted EMI emissions from an inverter-driven motor," *IEEE Trans. Power Electron.*, vol. 23, no. 1, pp. 282–290, Jan. 2008.
[19] G. Shen, D. Xu, L. Cao, and X. Zhu, "An improved control strategy for grid-connected voltage source inverters with an LCL filter," *IEEE Trans. Power Electron.*, vol. 23, no. 4, pp. 1899–1906, Jul. 2008.

Dong Jiang, photograph and biography not available at the time of publication.

Authorized licensed use limited to: University of Florida. Downloaded on December 30,2020 at 05:33:09 UTC from IEEE Xplore. Restrictions apply.

Rixin Lai, photograph and biography not available at the time of publication.

Fei (Fred) Wang (S'85–M'91–SM'99–F'10) received the B.S. degree from Xi'an Jiaotong University, Xi'an, China, and the M.S. and Ph.D. degrees from the University of Southern California, Los Angeles, in 1982, 1985, and 1990, respectively, all in electrical engineering.

He was a Research Scientist in the Electric Power Lab, University of Southern California, from 1990 to 1992. He joined the GE Power Systems Engineering Department, Schenectady, NY, as an Application Engineer in 1992. From 1994 to 2000, he was a Senior Product Development Engineer with GE Industrial Systems, Salem, VA. During 2000 to 2001, he was the Manager of Electronic and Photonic Systems Technology Lab, GE Global Research Center, Schenectady, NY and Shanghai, China. In 2001, he joined the Center for Power Electronics Systems (CPES) at Virginia Tech, Blacksburg, as a Research Associate Professor and became an Associate Professor in 2004. From 2003, he also served as the CPES Technical Director. Since 2009, he has been with The University of Tennessee and Oak Ridge National Lab, Knoxville, TN as a Professor and Condra Chair of Excellence in Power Electronics. His research interests include power electronics, power systems, controls, electric machines and motor drives.

Dr. Wang is a founding member of the new multi-university NSF/DOE Engineering Research Center on Ultra-wide-area Resilient Electric Energy Transmission Networks (CURENT) led by The University of Tennessee.

Fang Luo, photograph and biography not available at the time of publication.

Shuo Wang (S'03–M'06–SM'07) received the Ph.D. degree from the Center for Power Electronics Systems (CPES), Virginia Tech, Blacksburg, in 2005.

He has been with the Department of Electrical and Computer Engineering, the University of Texas at San Antonio (UTSA), since 2010. Before he joined UTSA, he was with GE Aviation Systems in Ohio and CPES at Virginia Tech. He has published around 90 journal and conference papers and is a holder of 5 US patents.

Dr. Wang received two IEEE paper awards and is an Associate Editor for IEEE TRANSACTION ON INDUSTRY APPLICATIONS.

Dushan Boroyevich (S'81–M'86–SM'03–F'06) received the Dipl. Ing. degree from the University of Belgrade in 1976, the M.S. degree from the University of Novi Sad in 1982, both in Yugoslavia, and the Ph.D. degree from Virginia Polytechnic Institute and State University (Virginia Tech), Blacksburg, in 1986.

From 1986 to 1990, he was an Assistant Professor and Director of the Power and Industrial Electronics Research Program in the Institute for Power and Electronic Engineering, University of Novi Sad, and later, acting Head of the Institute. He then joined the Bradley Department of Electrical and Computer Engineering at Virginia Tech as an Associate Professor. He is now the American Electric Power Professor at the department and co-director of the Center for Power Electronics Systems (CPES). His research interests include multi-phase power conversion, electronic power distribution systems, power electronics systems modeling and control, and integrated design of power converters.

Dr. Boroyevich received the IEEE William E. Newell Power Electronics Technical Field Award. He is 2011-12 President of IEEE Power Electronics Society.

Authorized licensed use limited to: University of Florida. Downloaded on December 30,2020 at 05:33:09 UTC from IEEE Xplore. Restrictions apply.